

# An analysis of the origin and propagation of the multiple coronal mass ejections of 2010 August 01

R.A. Harrison<sup>1</sup>, J.A. Davies<sup>1</sup>, C. Möstl<sup>2,3,4</sup>, Y. Liu<sup>4,5</sup>, M. Temmer<sup>2,3</sup>, M.M. Bisi<sup>6,7</sup>, J.P. Eastwood<sup>8</sup>, C.A. de Koning<sup>9</sup>, N. Nitta<sup>10</sup>, T. Rollett<sup>2,3</sup>, C.J. Farrugia<sup>11</sup>, R.J. Forsyth<sup>8</sup>, B.V. Jackson<sup>7</sup>, E.A. Jensen<sup>12</sup>, E.K.J. Kilpua<sup>13</sup>, D. Odstrcil<sup>14</sup>, D.F. Webb<sup>15</sup>

<sup>1</sup> RAL Space, Rutherford Appleton Laboratory, UK

<sup>4</sup> Space Sciences Laboratory, University of California, USA

<sup>7</sup> Center for Astrophysics and Space Sciences, University of California, San Diego, USA

<sup>10</sup> Solar & Astrophysics Lab., Lockheed Martin Advanced Technology Centre, USA

<sup>13</sup> Department of Physics, University of Helsinki, Finland

<sup>2</sup> Institute of Physics, University of Graz, Austria

<sup>5</sup> State Key Laboratory of Space Weather, Beijing, China

<sup>8</sup> The Blackett Laboratory, Imperial College London, London, UK

<sup>11</sup> Space Science Center and Department of Physics, University of New Hampshire, USA

<sup>14</sup> George Mason University/NASA Goddard Space Flight Center, Greenbelt, USA

<sup>3</sup> Space Research Institute, Austrian Academy of Sciences, Graz, Austria

<sup>6</sup> Institute of Mathematics and Physics, Aberystwyth University, Wales, UK

<sup>9</sup> NOAA Space Weather Prediction Center, Boulder Colorado, USA

<sup>12</sup> Planetary Science Institute, 1700 East Fort Lowell, Suite 106, Tucson, AZ, USA

<sup>15</sup> Institute for Scientific Research, Boston College, USA

On 2010 August 01, the northern solar hemisphere underwent significant activity that involved a complex set of active regions near central meridian with, nearby, two large prominences, and other more distant active regions. This activity culminated in the eruption of four major coronal mass ejections (CMEs), effects of which were detected at Earth and other solar system bodies. Recognising the unprecedented wealth of data from the wide range of spacecraft that were available - providing the potential for us to explore methods for CME identification and tracking, and to assess issues regarding onset and planetary impact - we present a comprehensive analysis of this sequence of CMEs. We show that, for three of the four major CMEs, onset is associated with prominence eruption, while the remaining CME appears to be closely associated with a flare. Using instrumentation onboard the STEREO spacecraft, three of the CMEs could be tracked out to elongations beyond 50°; their directions and speeds have been determined by various methods, not least to assess their potential for Earth impact. The analysis techniques that can be applied to the other CME, the first to erupt, are more limited since that CME was obscured by the subsequent, much faster, event before it had propagated far from the Sun; we discuss the speculation that these two CMEs interact. The consistency of the results, derived from the wide variety of methods applied to such an extraordinarily complete dataset, has allowed us to converge on robust interpretations of the CME onsets and their arrivals at 1 AU. These are reported fully by Harrison *et al.* (2012) and summarised here.

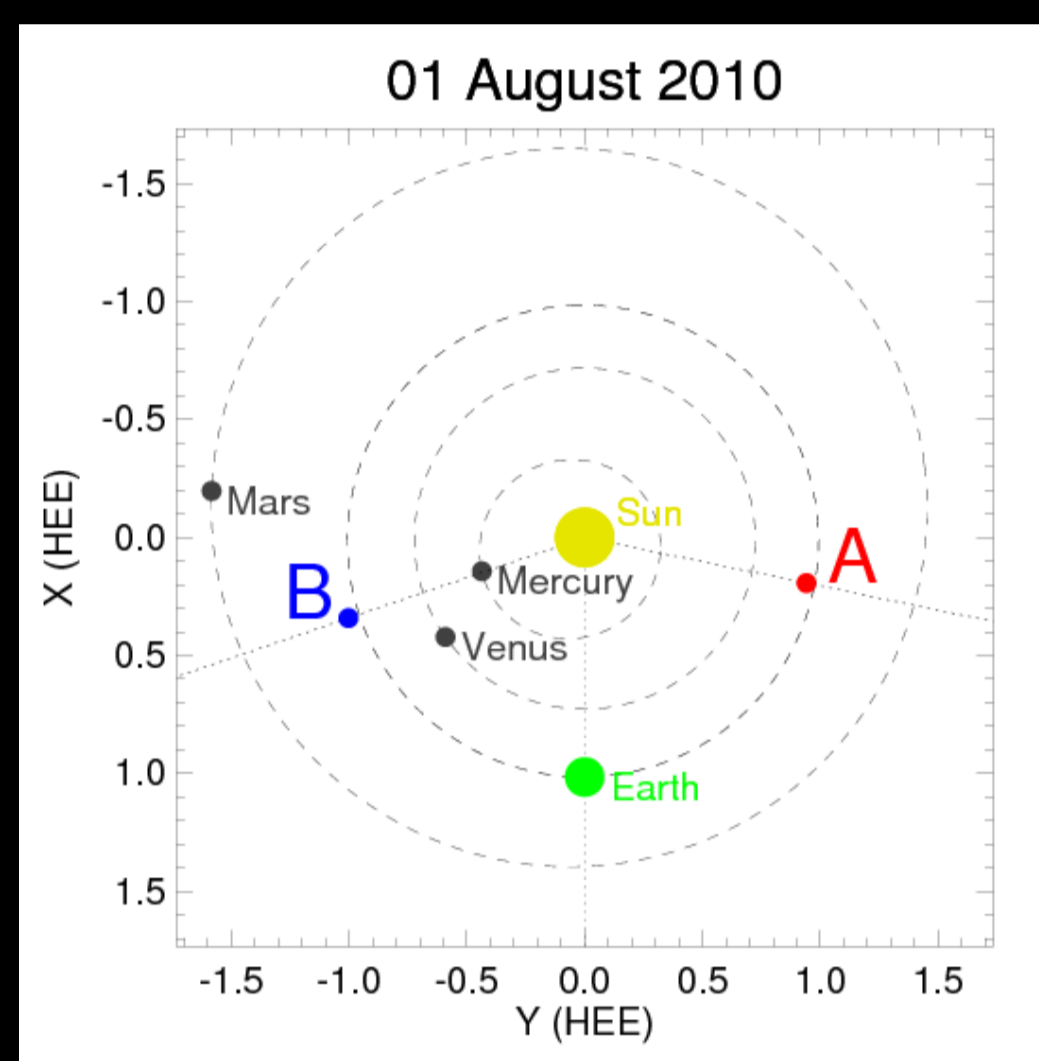


**Figure 1:** Locations of the STEREO-A and -B spacecraft, and the inner planets (Mercury, Venus, Earth, and Mars) in the Heliocentric Earth Ecliptic (HEE) X-Y plane on 2010 August 01 (see 'Where is STEREO?' web tool: <http://stereo-ssc.nascom.nasa.gov/where/>).

**Figure 2:** Six selected HI-1A images from 2010 August 01 in each of two formats, background-subtracted (upper six panels) and difference (lower six panels). Times are given on each panel. Elongation angle contours are overlaid on the first image of each format. Signatures of Venus and Mercury (at 10° and 20° elongation in the ecliptic, respectively) are evident in each image, and the Sun (centred at 0° elongation) is just off the centre right of each image. CMEs L, M, A and B are identified on the difference images.

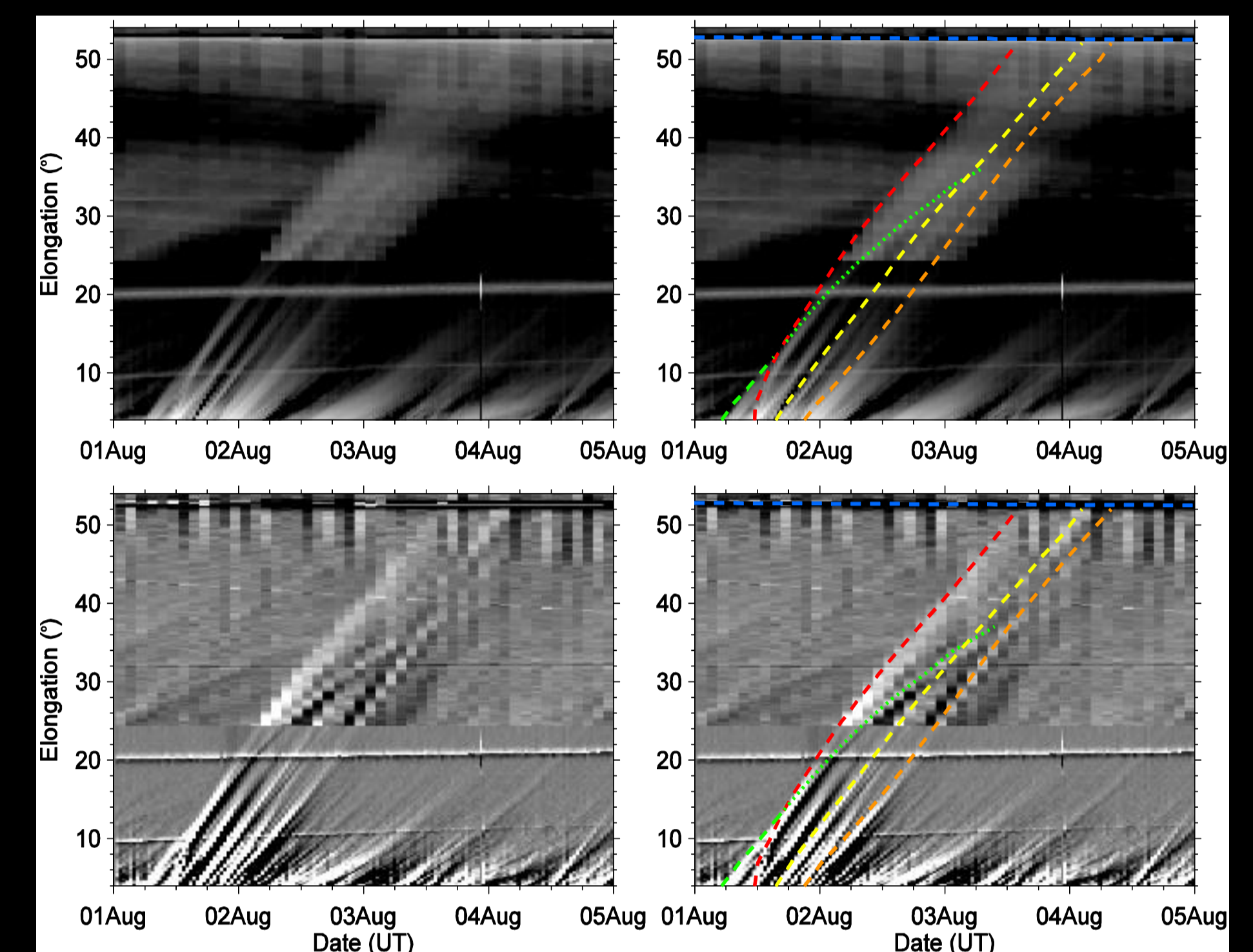
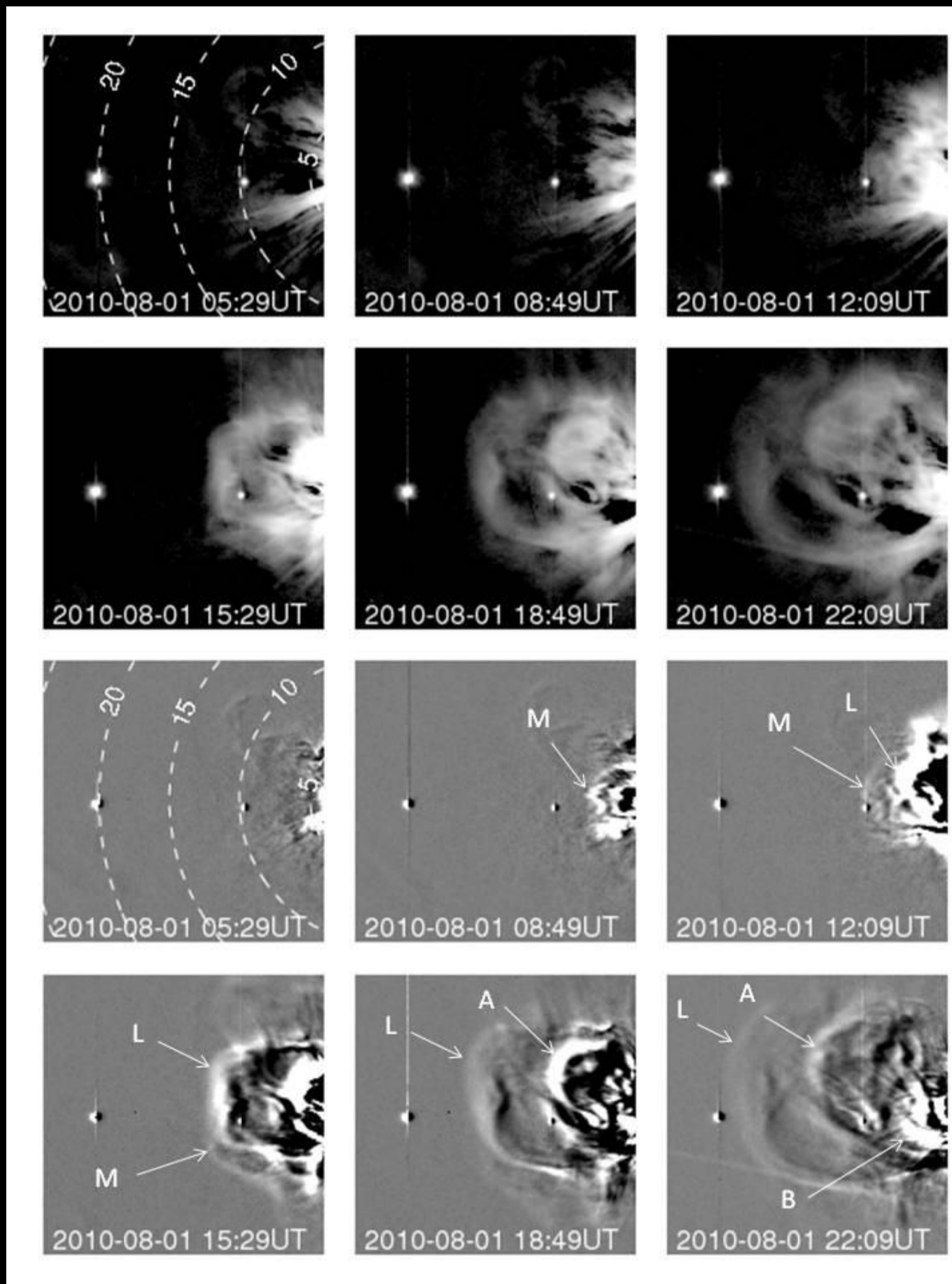


**Figure 3:** Time-elongation maps (I-maps) covering the interval 2010 August 01 to 05, constructed from HI-1A and HI-2A background-subtracted (upper panels) and difference (lower panels) observations extending from 4° to 54° elongation along the ecliptic. HI-1A data are plotted out to 24° elongation, HI-2A data therefrom. Right-hand panels show tracks corresponding to CMEs M, L, A, and B (marked in green, red, yellow, and orange, respectively). Near-horizontal signatures of Mercury, Venus, and Earth can be seen at elongations of 10°, 20°, and 53°, respectively; the latter is marked by a dashed blue line.

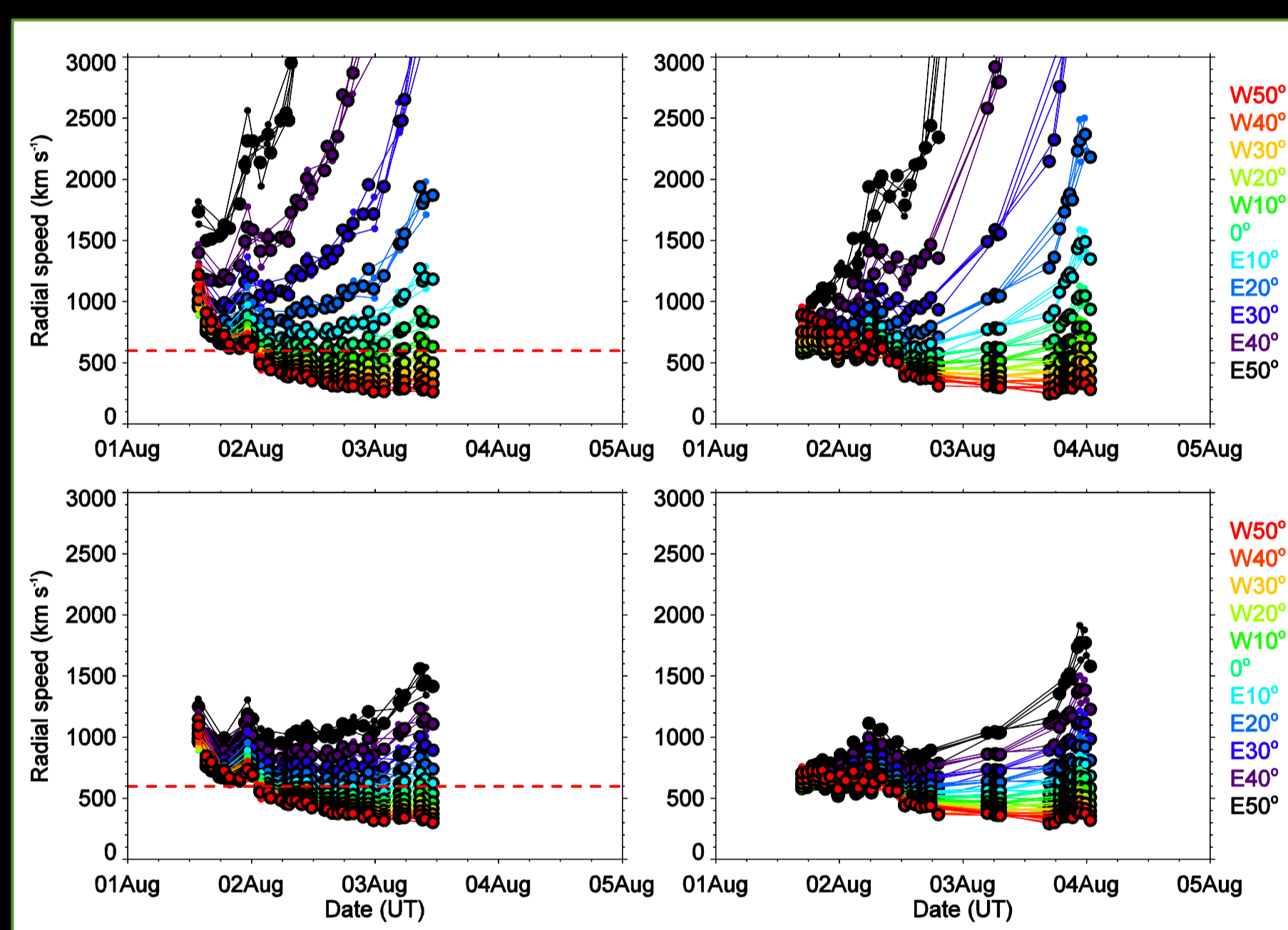


**Figure 4:** Radial speed profiles derived for CME L (left-hand panels) and CME A (right-hand panels), for a set of 11 fixed longitudes ranging from E50° to W50°, in steps of 10°, for both the Fixed Phi (FP; top panel) and Harmonic Mean (HM; bottom panel) geometric models. For each (colour-coded) longitude, six time series are plotted, one for each of the five sets of manually-selected points (marked with small dots), and the other indicating the average radial speed profile (large dots). For CME L (left-hand panels), a red dashed line indicates a speed of 600 km s<sup>-1</sup>, that being the solar wind speed measured by the near-Earth Wind spacecraft after the arrival of the principal shock associated with CME L. These fits are especially useful for fast CMEs, allowing an analysis of deceleration and the selection of physically meaningful velocity profiles.

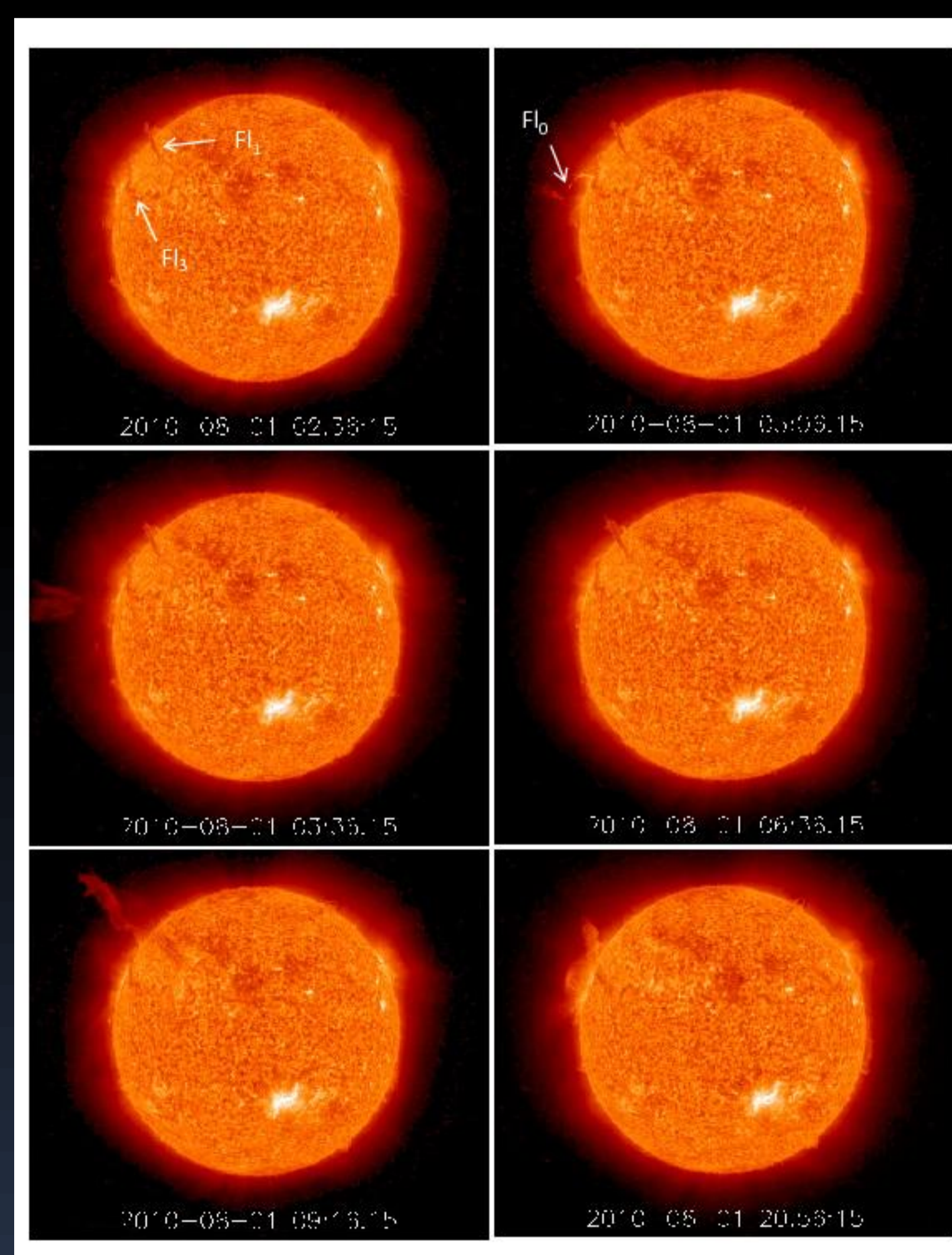


**Figure 5:** A selection of six EUVI images, taken by the STEREO-A spacecraft in the He II 304 Å emission line on 2010 August 01, in each case with the time of the exposure indicated. The locations of the two major filaments, F<sub>1</sub> and F<sub>2</sub>, are marked as is a filament on the east limb (F<sub>0</sub>). The ecliptic plane corresponds, approximately, to a horizontal line across the centre of each image.

**Figure 7:** Magnetic field and solar wind proton bulk parameters observed by Wind with 2-minute time resolution during the interval 2010 August 03 00:00 UT to 2010 August 06 00:00 UT. The top panel presents total magnetic field strength (black) and the magnetic field X and Y components in Geocentric Solar Ecliptic (GSE) coordinates, B<sub>x</sub> in red and B<sub>y</sub> in green. The second panel presents B<sub>z</sub> (GSE), in blue. The third, fourth, fifth, and sixth panels present proton speed, proton density, proton temperature, and proton beta, respectively (the latter being the ratio of plasma to magnetic pressure). The bottom panel presents the geomagnetic Kp (blue histogram) and Dst indices (green). A black vertical line on each panel marks the shock arrival at 17:05 UT on August 03. Shaded regions M1 to M3 demarcate magnetic flux ropes. Dashed red vertical lines correspond to the predicted arrival times of CMEs L, A and B; solid red horizontal lines indicate both the uncertainty in this timing estimate and the estimated CME speed. D1 marks a density enhancement at the rear of M2 and D2, possibly filament material (Möstl *et al.* 2012).

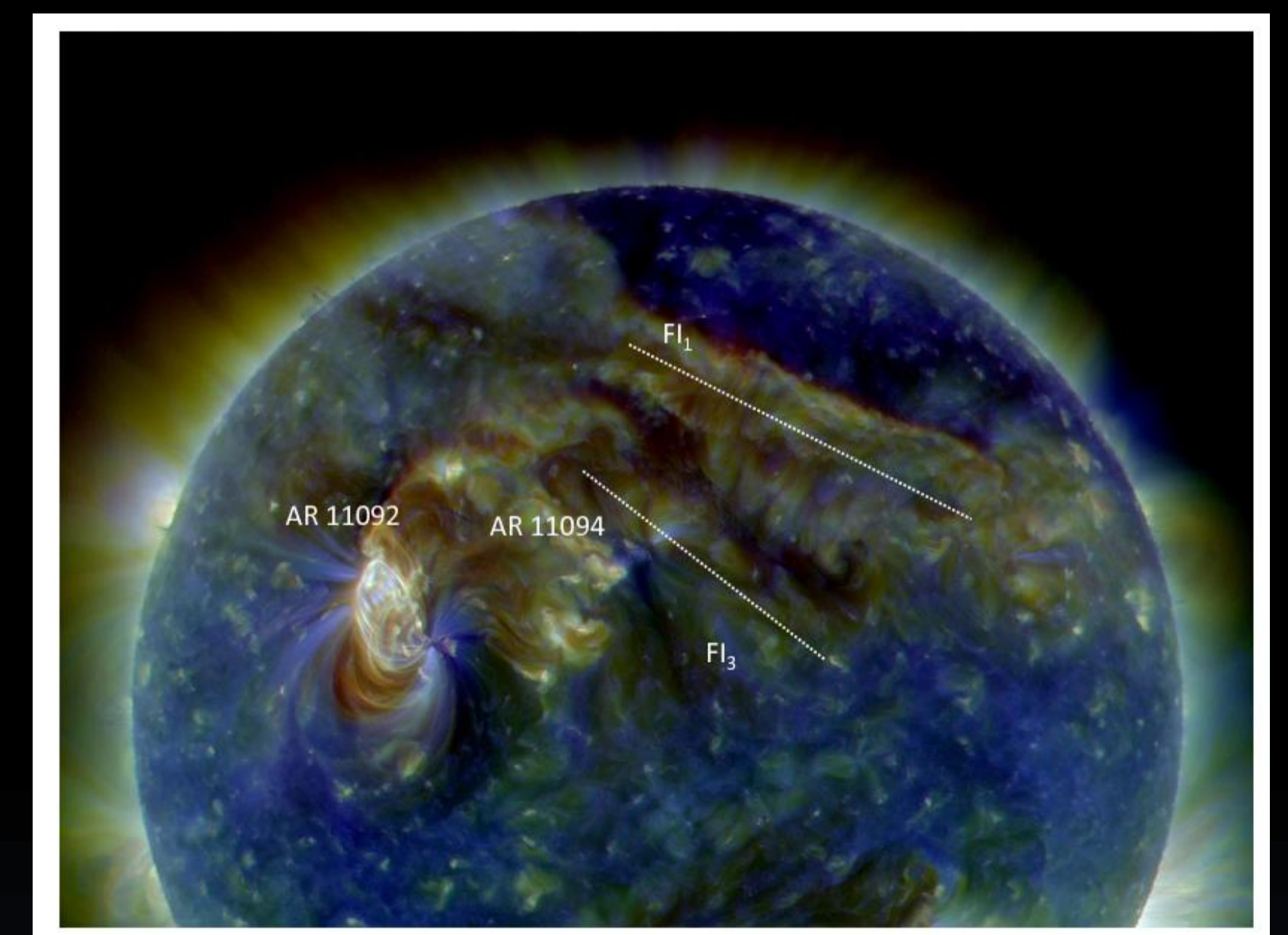


**Figure 6:** SDO/AIA EUV image of the solar disc taken at 12:13 UT on 2010 August 01, with the salient features marked, as identified by Schrijver & Title (2011).

## Summary and Conclusions:

- The complexity of the solar atmosphere on 1 August 2010 resulted in the launch of four major Earth-directed CMEs in quick succession. Despite this, there was considerable success in distinguishing between the distinct events, and modelling their kinematic properties, and, hence, predicting (albeit after the event) an arrival time at Earth. This was despite the fact that the two STEREO spacecraft were separated from Earth by ~80°, which might be considered to be past optimum viewing geometry for Earth-directed CMEs.

- The association between the phenomena occurring on the solar surface and the CMEs is not necessarily straightforward. This can limit the use of solar surface observations for predicting the CME propagation directions. Three of the CMEs had close associations with prominence eruptions with little or no associated flare activity. The fourth CME was associated with a modest flare, although it appeared to be located to one side of the CME source region.

- The first CME was subsumed by a second, much faster CME, which was initially travelling at a speed in excess of 1500 km s<sup>-1</sup>. Gauging the speed of that event required a unique modification to the standard HM and FP analysis of the STEREO/HI data. The two subsequent CMEs were propagating at speeds between 500 and 700 km s<sup>-1</sup>, and were well suited to the standard constant speed HM and FP analyses. The three resultant CMEs (the first of which corresponds to the merged initial pair of CMEs) were found to be propagating close enough to the Sun-Earth line to suggest an Earth impact. Their arrivals at Earth were associated with a substantial shock and two clear magnetic clouds. Comparison of predicted (after the event) and observed CME arrivals at Earth showed differences of less than 7 hr in all cases. Note that traces for these events in the time-elongation map actually cross the path of Earth; we actually see them arrive at Earth.

- The lack of obvious Earth-impacting events as viewed by SOHO/LASCO during this interval demonstrates that Earth-orbit is not the best vantage point for analysing Earth-directed CMEs.

## References:

Harrison, Davies, Möstl *et al.*, ApJ, 2012, in press  
Möstl *et al.*, ApJ, 2012, in preparation  
Schrijver and Title, 2011, J. Geophys. Res. 116, A04108